

**Disclosures.** M. K. Andrew, GSK: Grant Investigator, Research grant. Pfizer: Grant Investigator, Research grant. sanofi pasteur: Grant Investigator, Research grant. T. F. Hatchette, GSK: Grant Investigator, Research grant. Pfizer: Grant Investigator, Research grant. Abbvie: Consultant, Speaker honorarium. J. McElhane, GSK: Scientific Advisor, Speaker honorarium. sanofi pasteur: Scientific Advisor, Speaker honorarium. A. McGeer, GSK: Grant Investigator, Research grant. Hoffman La Roche: Grant Investigator, Research grant. sanofi pasteur: Grant Investigator, Research grant. A. Poirier, sanofi pasteur: Investigator, Research grant. Actelion: Grant Investigator, Research grant. J. Powis, GSK: Grant Investigator, Research grant. Merck: Grant Investigator, Research grant. Roche: Grant Investigator, Research grant. Synthetic Biologics: Investigator, Grant recipient. M. Semret, GSK: Grant Investigator, Research grant. Pfizer: Grant Investigator, Research grant. S. Trotter, CIHR: Grant Investigator, Research grant. S. A. McNeil, GSK: Grant Investigator, Research grant. Pfizer: Grant Investigator, Research grant. Merck: Collaborator and Consultant, Contract clinical trials and Speaker honorarium. Novartis: Collaborator, Contract clinical trials. sanofi pasteur: Collaborator, Contract clinical trials.

**993. Combining Key Residues of the Russian and US Live-Attenuated Influenza Viruses for a More Attenuated Virus**

Andrew Smith, MD/PhD Candidate<sup>1</sup>; Laura Rodriguez-Garcia, PhD<sup>1</sup>; Maya El Ghouayel, MHS, MD Candidate<sup>2</sup>; Luis Martinez-Sobrido, PhD<sup>1</sup> and Stephen Dewhurst, PhD<sup>1</sup>; <sup>1</sup>Department of Microbiology and Immunology, University of Rochester Medical Center, Rochester, New York, <sup>2</sup>University of Rochester School of Medicine and Dentistry, Rochester, New York

**Session:** 130. Adult and Pediatric Influenza Vaccine

**Friday, October 5, 2018: 12:30 PM**

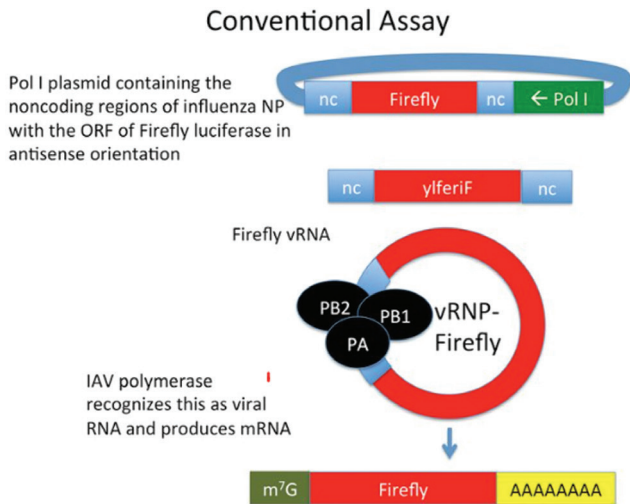
**Background.** The Live Attenuated Influenza Virus (LAIV) used in the United States is based on the cold-passaged A/AnnArbor/6/60 strain (AA). An alternative LAIV (Len), developed from the cold-passaged A/Leningrad/134/17/57 strain, has also been used in some countries outside the United States. Recent concerns with the efficacy and safety of the current US LAIV warrant the development of an improved LAIV.

**Methods.** We used *in vitro* minireplicon and multicycle viral growth assays to analyze the combined effects of polymerase mutations from LAIV (AA) and LAIV (Len) on the phenotype of PR8. Mini-replicon assays were performed in HEK-293T cells with firefly luciferase under the control of the influenza virus NP promoter; we controlled for cell density with a constitutively active Renilla luciferase. Multicycle growth curve experiments were performed at 33°C, 37°C, and 39°C in MDCK cells with an m.o.i. of 0.001. Mean values for triplicate infections at 12, 24, 48, and 72 hours were plotted as TCID<sub>50</sub>/mL.

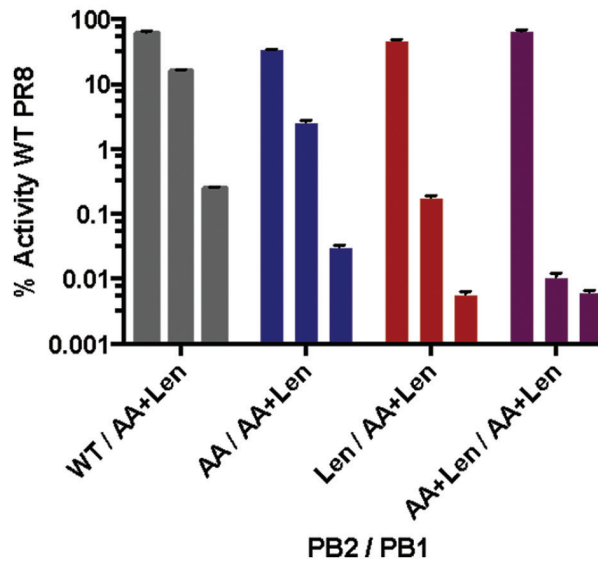
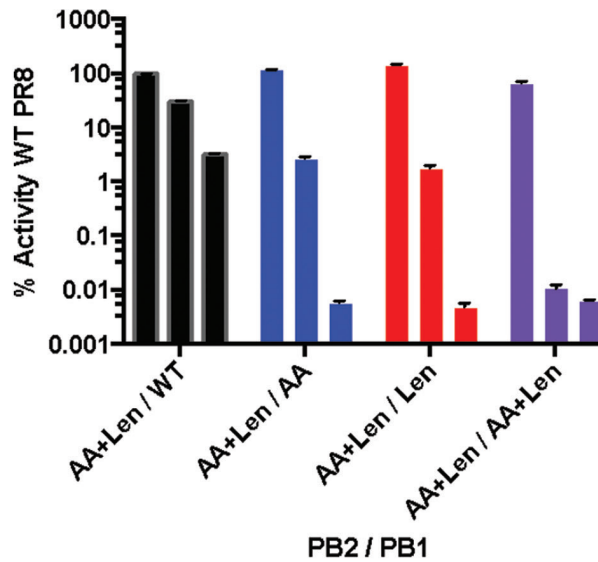
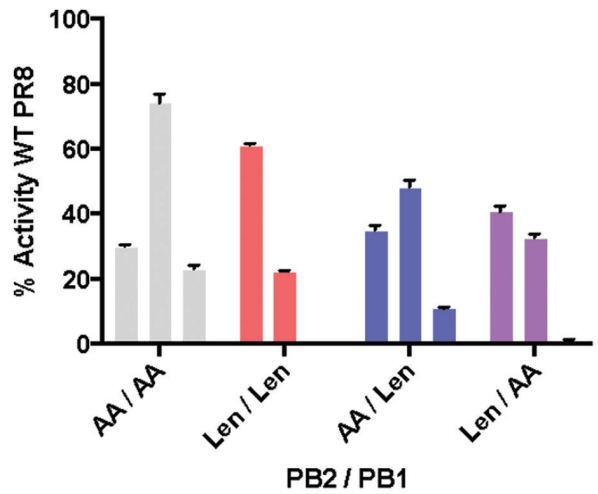
**Results.** Control experiments showed replication of PR8 (AA) and PR8 (Len) in MDCK cells was significantly decreased as compared with WT PR8 at 37°C and 39°C at 24–48 hour time points, but not at 33C (the temperature of nasal passages). We found that polymerase activity was up to 3 logs more temperature-sensitive (ts) at 37°C and 39°C with the combined Len and AA mutations using the mini-replicon assay. In the growth curve experiments, the combined Len and AA mutations conferred up to a 4-log decrease in replication levels at 37°C as compared with PR8 (Len) and an even greater decrease compared with PR8 (AA).

**Conclusion.** Our findings suggest combining the AA and Len LAIV polymerase mutations decreases LAIV replication at body temperature (37°C), as compared with either LAIV alone. This could be useful in developing an improved LAIV that is safer in vulnerable hosts (e.g., children under the age of 2 who may be vulnerable to wheezing), while also permitting dose escalation that might result in greater efficacy.

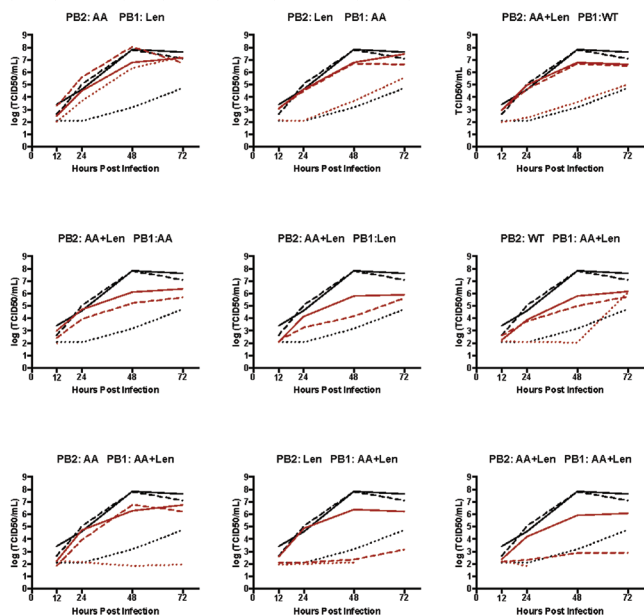
**Minireplicon assay.**



**Polymerase activity of combination mutants.**



**Multicycle replication kinetics of combination mutants (red) against PR8 Len (black) at 33C (solid), 37C (dashed) and 39C (dotted).**



**Disclosures.** All authors: No reported disclosures.

**994. AS03-Adjuvanted H5N1 Avian Influenza Vaccine Modulates Early Innate Immune Signatures in Peripheral Blood Mononuclear Cells**

Leigh Howard, MD, MPH<sup>1</sup>; Johannes Goll, M.S.<sup>2</sup>; Travis Jensen, B.S.<sup>2</sup>; Heather Hill, MS<sup>3</sup>; Casey Gelber, MS<sup>2</sup>; C. Buddy Creech, MD, MPH, FPIDS<sup>4</sup> and Kathryn Edwards, MD, FIDSA<sup>3</sup>; <sup>1</sup>Pediatrics, Vanderbilt University Medical Center, Nashville, Tennessee, <sup>2</sup>The EMMES Corporation, Rockville, Maryland, <sup>3</sup>EMMES Corporation, Rockville, Maryland, <sup>4</sup>Vanderbilt University School of Medicine, Nashville, Tennessee, <sup>5</sup>Department of Pediatrics, Division of Pediatric Infectious Diseases, Vanderbilt University School of Medicine, Nashville, Tennessee

**Session:** 130. Adult and Pediatric Influenza Vaccine  
**Friday, October 5, 2018: 12:30 PM**

**Background.** Influenza A/H5N1 vaccines have been poorly immunogenic. Addition of Adjuvant System 03 (AS03) markedly enhances immune responses, but the mechanisms of this enhancement are unclear.

**Methods.** We compared gene expression in peripheral blood mononuclear cells (PBMCs) between recipients of AS03-adjuvanted and unadjuvanted inactivated split-virus H5N1 vaccine on days 1, 3, 7, and 28 postvaccination. We used a systems vaccinology approach to assess functional classifications of differentially expressed (DE) genes between the two vaccine groups, identify DE genes that correlate with serologic responses, and compare these findings with previous cell-specific assessments.

**Results.** AS03-adjuvanted vaccine induced the strongest differential gene expression signals on day 1 after vaccination (Figure 1). Multiple innate immune signaling pathways were activated, including the interferon, JAK-STAT, and TNF pathways, and FC gamma receptor (Fc<sub>γ</sub>R) mediated phagocytosis. Immune pathways specific for antigen processing and presentation and influenza A responses were also enriched. Early differential expression of several signal transduction (day 1) and immunoglobulin (day 7) genes were predictive of peak HAI titer (Figure 2). Compared with cell-specific responses, DE gene, and immunologic pathways of PBMCs were most similar to innate immune cell subsets. However, several pathways were unique to PBMCs, and several cell-type-specific pathways, particularly from neutrophils, were absent in PBMCs (Figure 3).

**Conclusion.** Transcriptomic analysis of PBMCs after AS03-adjuvanted H5N1 vaccination revealed early differential regulation of multiple innate immune signaling pathways and enrichment of pathways involved in antigen presentation and influenza immune responses. Early expression of several genes was associated with peak HAI responses, suggesting a potential role for application of these signatures in earlier determination of vaccine responses. While PBMC and immune cell-specific results shared key innate immune signals, unique signals were identified by either approach.

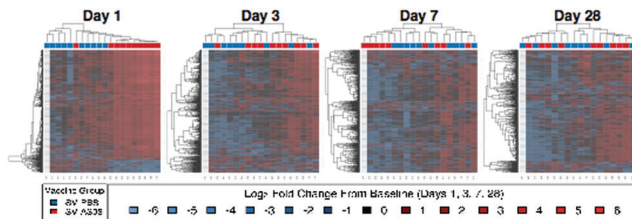


**Figure 1.** Heatmaps of baseline log<sub>2</sub> fold change signals for 474 DE differential genes (SV-AS03 group compared to the SV-PV5 group) identified in PBMCs at Day 1 for each of the 4 post-vaccination time points (red: upregulated from baseline, blue: downregulated from baseline). Dendrograms were obtained using complete linkage clustering of uncentered pairwise Pearson correlation distances between log<sub>2</sub> fold changes in log<sub>2</sub> fragment counts per million.

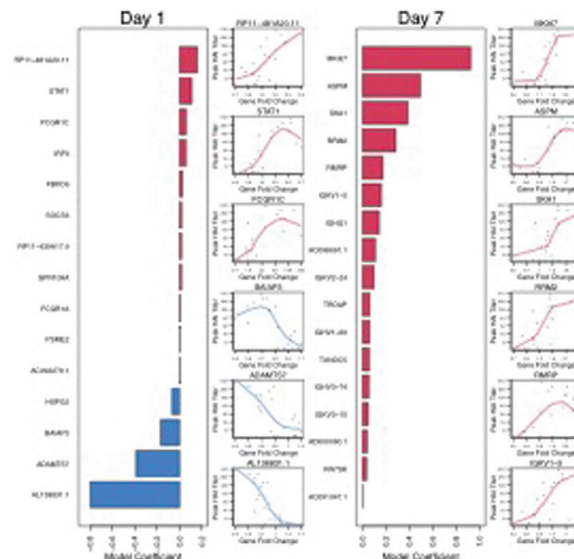


**Figure 2.** Correlation of day 1 and day 7 gene responses that best predicted later peak log<sub>2</sub> HAI titer. The bar plots represent the coefficients of the best predicted linear regression model. Scatterplots that summarize the correlation between peak log<sub>2</sub> HAI titer and log<sub>2</sub> gene fold change including locally weighted smoothed trend lines are shown for the top and bottom 3 genes for day 1 and the top 6 genes for day 7.

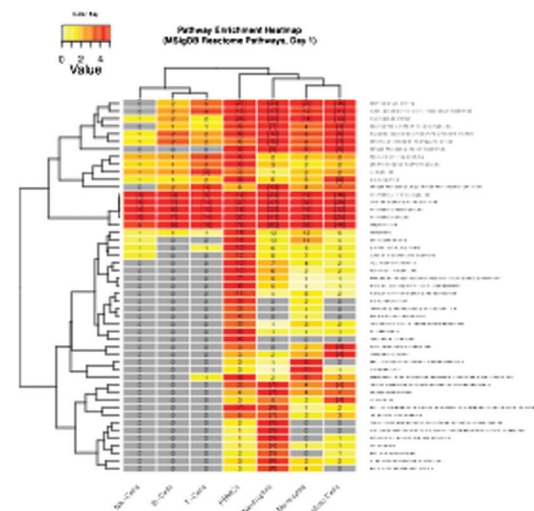


**Figure 3.** Comparison of Reactome pathway enrichment profiles between cell populations. Heatmap cell counts represent the number of DE genes in a pathway. Cells with numbers in brackets indicate significantly enriched pathways. Cells are color-coded by pathway enrichment score:  $-1 \times \log_{10}(\text{FDR-adjusted } p\text{-value})$  (dark red: highly enriched, light yellow: low level of enrichment). Dendrograms were obtained using complete linkage clustering of Euclidean distances between pathway enrichment scores.